Enabling NOMA in Overlay Spectrum Sharing in Hybrid Satellite-Terrestrial Systems

ANH-TU LE[ID][1]**, NHAT-DUY XUAN HA**[ID][1]**, DINH-THUAN DO**[ID][2,3,4]**, (Senior Member, IEEE),**
SUNEEL YADAV[ID][5]**, (Member, IEEE), AND BYUNG MOO LEE**[ID][6,7]**, (Senior Member, IEEE)**
[1]Faculty of Electronics Technology, Industrial University of Ho Chi Minh City, Ho Chi Minh City 700000, Vietnam
[2]Future Networking Research Group, Ton Duc Thang University, Ho Chi Minh City 700000, Vietnam
[3]Faculty of Electrical and Electronics Engineering, Ton Duc Thang University, Ho Chi Minh City 700000, Vietnam
[4]Department of Computer Science and Information Engineering, College of Information and Electrical Engineering, Asia University, Taichung 41354, Taiwan
[5]Department of Electronics and Communications Engineering, IIT Allahabad, Allahabad 211015, India
[6]Department of Intelligent Mechatronics Engineering, Sejong University, Seoul 05006, South Korea
[7]Department of Convergence Engineering for Intelligent Drone, Sejong University, Seoul 05006, South Korea

Corresponding authors: Dinh-Thuan Do (dodinhthuan@tdtu.edu.vn) and Byung Moo Lee (blee@sejong.ac.kr)

ABSTRACT In this paper, a hybrid satellite-terrestrial spectrum sharing system allows terrestrial secondary network to cooperate with a primary satellite network and to further provide higher spectrum efficiency. For massive connections design, we implement non-orthogonal multiple access (NOMA) technique to form cognitive radio based satellite-terrestrial (CR-NSHT) system relying on NOMA and further achieve more benefits compared with traditional schemes. The secondary network only remains its stable operation when the outage probability of such system is guaranteed, and thereby, to explore advantages of spectrum sharing opportunities. Considering Shadowed-Rician fading for satellite links, and Nakagami-*m* as well as Rician fading for terrestrial links, we derive the closed-form expressions of the outage probability to evaluate the performance of secondary network. We consider further system performance metrics including ergodic capacity, energy efficiency and multi-user scenarios. We also demonstrate the impacts of power allocation factors, transmit signal-to-noise ratio (SNR) at the source, parameters of satellite links, target rates, and fading severity parameters on the system performance. Numerical and simulation results validate our analysis and highlight the performance gains of the proposed schemes for CR-NSHT with relay link serving secondary network and direct link serving the primary network.

INDEX TERMS Hybrid satellite-terrestrial systems, cognitive radio, spectrum sharing, outage probability.

I. INTRODUCTION

To resolve the challenge of line-of-sight satellite communication systems blocked by heavy shadowing or obstacles [1], the authors in [2]–[6] has been studied a hybrid satellite-terrestrial system. In particular, a terrestrial relay is implemented in satellite communication systems to overcome challenges of large coverage and high data rate services. To enhance the wireless spectrum utilization, the satellite communication systems enable the cognitive radio (CR). Considering the benefits of the underlay CR scheme, cognitive hybrid satellite-terrestrial systems are proposed in [7], [8]. In such systems, the secondary users' spectrum access

The associate editor coordinating the review of this manuscript and approving it for publication was Qinghua Guo[ID].

opportunities are limited by the tolerable interference level which is allowed by the primary user. The performance analyses of the primary and secondary networks depend on interference coordination and such issue is considered as one of the key parameters to control the quality of service (QoS) of the primary network in the context of underlay transmission mode. In the overlay mode of CR network reported in [9], the secondary users help the primary transmission through cooperative relaying protocols related to spectrum access. In [10], the authors analyzed an overlay CR architecture in hybrid satellite-terrestrial networks to exhibit its performance. The authors in [11] investigated a novel cognitive hybrid satellite-terrestrial model including two cognitive relays which are enabled to forward their received signal to a mobile user successively. The secrecy

TABLE 1. Comparison of proposed system with related studies.

Context	Cooperative Relay Network	Relay Protocol	NOMA	Cognitive Radio	Outage probability of System	Diversity order	Ergodic Capacity	Multiple Users
This Work	Yes	DF	Yes	Yes	Yes	Yes	Yes	Yes
[11]	Yes	AF	No	Yes	No	No	Yes	No
[14]	Yes	AF	Yes	Yes	Yes	Yes	No	No
[30]	Yes	DF	Yes	Yes	Yes	No	Yes	No
[31]	No	No	Yes	Yes	Yes	No	No	No
[32]	Yes	AF	Yes	Yes	Yes	Yes	No	No

outage probability of the hybrid satellite-terrestrial network was analyzed to indicate the secrecy performance by introducing the closed-form formula for the single-relay selection and baseline round-robin scheduling modes [12]. By using Vickrey auction to achieve an efficient secondary relay selection, a cooperative spectrum sharing scheme is examined in the scenario of a multi-potential secondary relay selection [13]. X. Zhang *et al.* studied the generalized shadowed-Rician fading for satellite links while Nakagami-*m* fading is adopted in terrestrial links. Further, the authors derived the closed-form outage probability expressions for both the primary and secondary users [14]. To get extra spectrum efficiency, non-orthogonal multiple access (NOMA) was introduced in [15]–[24]. In principle of NOMA, multiple users are permitted to share the same resource elements in signal processing domains including time, frequency, space, or code. These studies presented a lot of benefits such as massive connectivity and high spectral efficiency. The satellite systems have more beneficial by implementing NOMA to form NOMA-aided hybrid satellite-terrestrial systems (NHST) [25]. The authors in [25] developed the model to allow a user with better channel condition to operate as a relay node and forwards signal to other users. Therefore, the impacts of the masking effect of users with poor channel conditions can be avoided in circumstance of heavy shadowing. The authors in [26] introduced how NOMA benefits to hybrid satellite-terrestrial relay network. Such NSHT enhances ability of spectrum sharing in the manner of the underlay architecture. The work in [27] considered NSHT by applying both the decode-and-forward (DF) and amplify-and-forward (AF) protocols at the relay and the imperfection of channel state information (CSI) at all nodes. Furthermore, NOMA can be applied to edge computing and content caching in wireless networks to enable the emerging networks which provide high-quality services for users [28], [29].

The performance of NOMA based cooperative spectrum sharing in hybrid satellite-terrestrial networks is studied in many scenarios [30]–[32]. The authors in [31] considered the underlay CR-HSTN including a primary satellite source with its terrestrial receiver and the secondary transmitter (ST) with its pre-paired users on the ground. They derived a novel closed-form formula to exhibit the outage performance of secondary network in the existence of primary interference power constraint imposed by the adjacent primary satellite network. The recent work reported the

asymptotic outage performance of CR-HSTN at high signal-to-noise-ratio (SNR) to show performance of the primary and secondary networks, and thereby achieve the diversity orders [32]. Those studies show open problem which motive us to study in this article.

Inspired by the comparison presented in Table 1, a CR-NHST need be studied in this paper to enhance the spectrum utilization and tackle the fairness issue benefiting by exploiting NOMA with fixed power allocation approach. The contributions of this work are manifolds as follows

- First of all, we propose a CR-NHST system, where the secondary terrestrial network operates under the help of the base station in role of relay. Besides, the NOMA is adopted in system to show differences in outage performance of two-user model.
- Secondly, different performance of two users under overlay paradigm is examined by deriving expressions in the closed-form for outage probability, ergodic capacity and energy efficiency. We also present related analysis in case of multiple users which need more signal processing stages in such system. Our results indicated that main parameters need be adjusted to achieve the improvement in term of system performance.
- Thirdly, more insights in term of performance analysis are provided. Particularly, the asymptotic expressions of outage probability and diversity order are derived.
- Finally, the impacts of key parameters in the CR-NHST system are analyzed, and the superiority of the CR-NHST relying on NOMA scheme is proved to compare to conventional OMA-based satellite system in terms of outage and throughput performance.

The rest of this paper is organized as follows. Section II introduces the CR-NHST system model, reformulates signal to interference plus noise ratio (SINR), and gives channels model. In Section III, the exact expressions of outage probability are derived. Section IV present the extended case for multiple users in the considered system and Section V shows simulation results. Finally, conclusions are drawn in Section VI.

II. SYSTEM MODEL
Considering system model in Fig. 1, a CR-NHST includes the secondary network (SN) serving NOMA users. The SN comprises of a satellite transmitter (S), terrestrial base station (R), two user D_1, D_2 and the primary network with corresponding
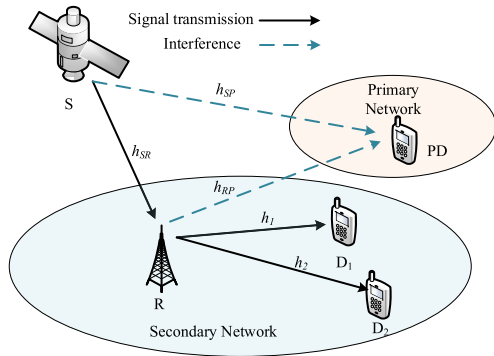
FIGURE 1. System model of CR-NHST system relying on NOMA.

TABLE 2. The main parameters of the system model.

Symbol	Description
h_{SR}	The channel coefficient from the satellite to the relay
h_{SP}	The channel coefficient from the satellite to the primary destination
h_{RP}	The channel coefficient from the relay to the primary destination
h_i	The channel coefficient between the relay and secondary user D_i, $i \in \{1, 2\}$
P_j	The transmit power at j, $j \in \{S, R\}$
$\bar{P}_j$	The maximum transmit power at j
P_D	The interference temperature constraint at PD
n_R, n_{D_i}	The additive white Gaussian noise(AWGN) at R and D_i with $\mathcal{CN}(0, \sigma_R^2)$ and $\mathcal{CN}(0, \sigma_i^2)$ respectively
x_i	The signals corresponding users D_i
a_i	the power allocation coefficients

primary destination PD. We will consider the situation of multiple users in section IV. Let such satellite be a GEO satellite and the terrestrial nodes be fixed service terminals. The base station and mobile users are single antenna nodes. We do not concern the Doppler spread at the terrestrial node due to static their nature. Therefore, the secondary transmitter (base station) performs for spectrum sharing opportunities to send signals to its intended secondary receivers. The main symbols and parameters can be clarified in table 2. The transmit power at S and R is constrained by [33]

$$P_j = \min\left(\bar{P}_j, \frac{P_D}{|h_{jP}|^2}\right). \quad (1)$$

In two-phase transmission from satellite to users, S sends the superposed signal $\sqrt{a_1 P_S}x_1 + \sqrt{a_2 P_S}x_2$ to R in the first phase. Following principle of NOMA, operation of such network is conditioned on $a_1 < a_2$ and $a_1 + a_2 = 1$. In the second phase, R forwards signals to two secondary destinations.

In the first phase, the received signal at R is given by

$$y_R = \left(\sqrt{a_1}x_1 + \sqrt{a_2}x_2\right)\sqrt{P_S}h_{SR} + n_R. \quad (2)$$

The signal to interference plus noise ratio (SINR) decoding x_2 is given by

$$\Gamma_{R,x_2} = \frac{P_S a_2 |h_{SR}|^2}{P_S a_1 |h_{SR}|^2 + \sigma_R^2}. \quad (3)$$

After applying SIC, the SINR computed at R is used for decoding signal x_1 and such SINR is given by

$$\Gamma_{R,x_1} = \frac{P_S a_1 |h_{SR}|^2}{\sigma_R^2}. \quad (4)$$

In the second phase, the relay transmits the signal to D_i with $i \in \{1, 2\}$. The received signal at D_i can be expressed as

$$y_{D_i} = \left(\sqrt{a_1}x_1 + \sqrt{a_2}x_2\right)\sqrt{P_R}h_i + n_{D_i}. \quad (5)$$

The SINR at D_2 used for decoding x_2 is calculated by

$$\Gamma_{D_2,x_2} = \frac{P_R a_2 |h_2|^2}{P_R a_1 |h_2|^2 + \sigma_2^2}. \quad (6)$$

Then, the SINR at D_1 for detecting x_2 is computed by

$$\Gamma_{D_1,x_2} = \frac{P_R a_2 |h_1|^2}{P_R a_1 |h_1|^2 + \sigma_1^2}. \quad (7)$$

Applying SIC, the SINR for decoding x_1 at D_1 is given by

$$\Gamma_{D_1,x_1} = \frac{P_R a_1 |h_1|^2}{\sigma_1^2}. \quad (8)$$

III. PERFORMANCE ANALYSIS
A. CHANNEL MODELS
Under Shadowed-Rician fading model for the satellite links, the probability density function (PDF) of $|h_{Sk}|^2$ with $k \in (R, P)$ is given by [3]

$$f_{|h_{Sk}|^2}(x) = \alpha_{Sk}e^{-\beta_{Sk}x}{}_1F_1(m_{Sk}; 1; \delta_{Sk}x), x > 0 \quad (9)$$

where $\alpha_{Sk} = \left(\frac{2b_{Sk}m_{Sk}}{2b_{Sk}m_{Sk}+\Omega_{Sk}}\right)^{m_{Sk}}/2b_{Sk}$, $\beta_{Sk} = 0.5b_{Sk}$ and $\delta_{Sk} = \Omega_{Sk}/(2b_{Sk})(2b_{Sk}m_{Sk}+\Omega_{Sk})$, with Ω_{Sk} and $2b_{Sk}$ denote the respective average power of the LOS and multipath components, m_{Sk} is the fading severity parameter and $_1F_1(.)$ is the confluent hypergeometric function of the first kind [41, Eq. 9.210.1]. In this paper, we consider arbitrary integer-valued fading severity parameter [34]. Then, we can simplify (9) as

$$f_{|h_{Sk}|^2}(x) = \alpha_{Sk}\sum_{n_{Sk}=0}^{m_{Sk}-1}\zeta_{Sk}(n_{Sk})x^{n_{Sk}}e^{-(\beta_{Sk}-\delta_{Sk})x}, \quad (10)$$

where $\zeta_{Sk}(n_{Sk}) = (-1)^{n_{Sk}}(1-m_{Sk})_{n_{Sk}}\delta_{Sk}^{n_{Sk}}/(n_{Sk}!)^2$ and $(.)_{n_{Sk}}$ is the Pochhammer symbol [41, p.xliii]. Thus, we can obtain the CDF of $|h_{Sk}|^2$ as

$$F_{|h_{Sk}|^2}(x) = 1 - \alpha_{Sk}\sum_{n_{Sk}=0}^{m_{Sk}-1}\zeta_{Sk}(n_{Sk})$$
$$\times \sum_{q=0}^{n_{Sk}}\frac{n_{Sk}!x^q e^{-(\beta_{Sk}-\delta_{Sk})x}}{q!(\beta_{Sk}-\delta_{Sk})^{n_{Sk}-q+1}} \quad (11)$$

The PDF and cumulative distribution function (CDF) of $|h_l|^2$ for $l \in \{RP, 1, 2\}$ are computed respectively as

$$f_{|h_j|^2}(x) = \left(\frac{m_j}{\lambda_j}\right)^{m_j}\frac{x^{m_j-1}e^{-\left(\frac{m_j}{\lambda_j}\right)x}}{\Gamma(m_j)} \quad (12)$$

and

$$
\begin{aligned}
F_{|h_l|^2}(x) &= \frac{\gamma\left(m_l, m_l x/\lambda_l\right)}{\Gamma\left(m_l\right)} \\
&= 1 - e^{-\frac{m_l x}{\lambda_l}} \sum_{n_l=0}^{m_l-1} \frac{x^{n_l}}{n_l!}\left(\frac{m_l}{\lambda_l}\right)^l,
\end{aligned} \tag{13}
$$

where $\gamma(.,.)$ is the lower incomplete gamma functions [41, 8.310.1], m_k and λ_k denote the fading severity and average power, respectively.

B. OUTAGE PERFORMANCE

1) OUTAGE PROBABILITY OF D_2

For target rates R_i, the OP of the secondary satellite network with relay link enabled. We deal with two kinds of fading channels in the secondary network, especially considering Nakagami-m and Rician fading environments for terrestrial links. The OP at user D_2 is expressed by

$$
\begin{aligned}
OP_{D_2} &= \Pr\left(\min\left(\Gamma_{R,x_2}, \Gamma_{D_1,x_2}, \Gamma_{D_2,x_2}\right) < \psi_{th_2}\right) \\
&= F_{\Gamma_{D_1,x_2}}\left(\psi_{th_2}\right) + \left(1 - F_{\Gamma_{D_1,x_2}}\left(\psi_{th_2}\right)\right) \\
&\quad \times \left(F_{\Gamma_{D_2,x_2}}\left(\psi_{th_2}\right) + F_{\Gamma_{R,x_2}}\left(\psi_{th_2}\right)\right. \\
&\quad \left. - F_{\Gamma_{D_2,x_2}}\left(\psi_{th_2}\right) F_{\Gamma_{R,x_2}}\left(\psi_{th_2}\right)\right),
\end{aligned} \tag{14}
$$

where $\psi_{th_i} = 2^{2R_i} - 1$ is the threshold SNR corresponding to target rates R_i for two users D_i.

Lemma 1: The term $F_{\Gamma_{D_i,x_2}}\left(\psi_{th_2}\right)$ can be expressed as (15), shown at the bottom of the next page.

 Proof: See Appendix A

Lemma 2: We can calculate $F_{\Gamma_{R,x_2}}\left(\psi_{th_2}\right)$ as (16), shown at the bottom of the next page.

 Proof: See Appendix B.

Finally, with the help of (15), (16) and after some manipulations, the closed-form expression of OP for D_2 is obtained as

$$
\begin{aligned}
OP_{D_2} &= 1 - \left(1 - F_{\Gamma_{R,x_2}}\left(\psi_{th_2}\right)\right) \\
&\quad \times \left(1 - F_{\Gamma_{D_2,x_2}}\left(\psi_{th_2}\right)\right)\left(1 - F_{\Gamma_{R,x_2}}\left(\psi_{th_2}\right)\right).
\end{aligned} \tag{17}
$$

2) OUTAGE PERFORMANCE OF D_1

In this section, we conduct the OP analysis of the secondary network of CR-NHST under NOMA scheme in the absence of direct R-D_1 link.

$$
\begin{aligned}
OP_{D_1} &= \Pr\left(\min\left(\Gamma_{R,x_1}, \Gamma_{D_1,x_1}\right) < \psi_{th_1}\right) \\
&= F_{\Gamma_{R,x_1}}\left(\psi_{th_1}\right) + F_{\Gamma_{D_1,x_1}}\left(\psi_{th_1}\right) \\
&\quad - F_{\Gamma_{R,x_1}}\left(\psi_{th_1}\right) F_{\Gamma_{D_1,x_1}}\left(\psi_{th_1}\right).
\end{aligned} \tag{18}
$$

Based on (1) and (4), we can write $F_{\Gamma_{R,x_1}}\left(\psi_{th_1}\right)$ as

$$
\begin{aligned}
F_{\Gamma_{R,x_1}}\left(\psi_{th_1}\right) &= 1 - \Pr\left(\frac{P_S a_1 |h_R|^2}{\sigma_R^2} > \psi_{th_1}\right) \\
&= 1 - \Pr\left(|h_{SR}|^2 > \frac{\psi_{th_1}}{\bar{\rho}_S a_1}, |h_{SP}|^2 < \frac{\rho_D}{\bar{\rho}_S}\right) \\
&\quad - \Pr\left(|h_{SR}|^2 > \frac{\psi_{th_1}|h_{SP}|^2}{\rho_D a_1}, |h_{SP}|^2 > \frac{\rho_D}{\bar{\rho}_S}\right).
\end{aligned} \tag{19}
$$

Similarly, with the help from Appendix B, it can be rewritten as

$$
\begin{aligned}
&F_{\Gamma_{R,x_1}}\left(\psi_{th_1}\right) \\
&= 1 - \alpha_{SR} \sum_{k_{SR}=0}^{m_{SR}-1} \zeta_{SR}\left(k_{SR}\right) e^{-\frac{\psi_{th_1}(\beta_{SR}-\delta_{SR})}{\bar{\rho}_S a_1}} \\
&\quad \times \sum_{l_{SR}=0}^{k_{SR}} \frac{k_{SR}!\left(\psi_{th_1}\psi_{th_1}/\bar{\rho}_S a_1\right)^{l_{SR}}}{l_{SR}!\left(\beta_R - \delta_R\right)^{k_{SR}-l_{SR}+1}} \left(1 - \sum_{k_{SP}=0}^{m_{SP}-1} \zeta_{SP}\left(k_{SP}\right)\right. \\
&\quad \left. \times \sum_{l_{SP}=0}^{k_{SP}} \frac{k_{SP}!\alpha_{SP}(\rho_D/\bar{\rho}_S)^{l_{SP}} e^{-\frac{\rho_D(\beta_{SP}-\delta_{SP})}{\bar{\rho}_S}}}{l_{SP}!\left(\beta_{SP} - \delta_{SP}\right)^{k_{SP}-l_{SP}+1}}\right) \\
&\quad - \sum_{k_{SR}=0}^{m_{SR}-1} \zeta_{SR}\left(k_{SR}\right) \sum_{k_{SP}=0}^{m_{SP}-1} \zeta_{SP}\left(k_{SP}\right) \sum_{l_{SR}=0}^{k_{SR}} \sum_{l_{SP}=0}^{k_{SP}+l_{SP}} \\
&\quad \times \frac{\alpha_{SP}\alpha_{SR}k_{SR}!\left(k_{SP}+l_{SP}\right)!\left(\rho_D/\bar{\rho}_S\right)^{l_{SP}}}{l_{SR}!l_{SP}!\left(\beta_{SR}-\delta_{SR}\right)^{k_{SR}-l_{SR}+1}} \\
&\quad \times e^{-\left(\frac{\psi_{th_1}(\beta_{SR}-\delta_{SR})}{\rho_D a_1}+(\beta_{SP}-\delta_{SP})\right)\frac{\rho_D}{\bar{\rho}_S}} \left(\frac{\psi_{th_1}}{\rho_D a_1}\right)^{l_{SR}} \\
&\quad \times \left(\frac{\psi_{th_1}\left(\beta_R - \delta_R\right)}{\bar{\rho}_D a_1} + \left(\beta_{SP} - \delta_{SP}\right)\right)^{l_{SP}-k_{SP}-l_{SP}-1}.
\end{aligned} \tag{20}
$$

Regarding the computation at R, $F_{\Gamma_{D_1,x_1}}\left(\psi_{th_1}\right)$ is given by

$$
\begin{aligned}
&F_{\Gamma_{D_1,x_1}}\left(\psi_{th_1}\right) \\
&= 1 - \sum_{n_1=0}^{m_1-1} \frac{e^{-\frac{\psi_{th_1}m_1}{a_1\bar{\rho}_R\lambda_1}}}{n_1!}\left(\frac{\psi_{th_1}m_1}{a_1\bar{\rho}_R\lambda_1}\right)^{n_1} \\
&\quad \times \left(1 - \sum_{n_{RP}=0}^{m_{RP}-1} \frac{e^{-\frac{m_{RP}\rho_D}{\lambda_{RP}\bar{\rho}_R}}}{n_{RP}!}\left(\frac{\rho_D m_{RP}}{\bar{\rho}_R\lambda_{RP}}\right)^{n_{RP}}\right) \\
&\quad - \sum_{n_1=0}^{m_1-1} \sum_{b_1=0}^{m_{RP}+n_1-1} \binom{m_{RP}+n_1-1}{m_{RP}-1}\left(\frac{\rho_D m_{RP}}{\bar{\rho}_R\lambda_{RP}}\right)^{m_{RP}} \\
&\quad \times \left(\frac{\psi_{th_1}m_1}{a_1\lambda_1\bar{\rho}_R}\right)^{n_1} \frac{e^{-\frac{\psi_{th_1}\lambda_{RP}m_1+a_1 m_{RP}\lambda_1\rho_D}{a_1\lambda_1\lambda_{RP}\bar{\rho}_R}}}{b_1!} \\
&\quad \times \left(\frac{a_1\lambda_1\lambda_{RP}\bar{\rho}_R}{\psi_{th_1}m_1\lambda_{RP}+a_1 m_{RP}\lambda_1\rho_D}\right)^{m_{RP}+n_1-b_1}.
\end{aligned} \tag{21}
$$

Finally, putting (20) and (21) into (18) OP_{D_2} can be obtained as (22), shown at the bottom of the next page.

Remark 1: Although the exact OP expression of CR-NHST based on (22) is useful and provide several insights from numerical plots, it is too complex to predict main impacts on system performance of the secondary network. Fortunately, transmit SNR at the satellite plays an important role in outage performance. Therefore, a further metric is necessary to highlight performance improvement of such CR-NHST. For this, we consider throughput performance in the following section. This is ergodic capacity in delay-limited mode.[1]

---

[1]These metrics are enough to confirm advantage of NOMA in such CR-NHST system. We do not want to study ergodic capacity in delay tolerant mode. Our work provides similar metrics reported in [10].

$$
\begin{aligned}
F_{\Gamma_{D_i,x_2}}\left(\psi_{th_2}\right) = {} & 1 - \sum_{n_i=0}^{m_i-1} \frac{e^{-\frac{\psi_{th_2}m_2}{\left(a_2-a_1\psi_{th_2}\right)\bar{\rho}_R\lambda_i}}}{n_i!}\left(\frac{\psi_{th_2}n_i}{\left(a_2-a_1\psi_{th_2}\right)\bar{\rho}_R\lambda_i}\right)^{n_i} \\
& + \sum_{n_i=0}^{m_i-1}\sum_{n_{RP}=0}^{m_{RP}-1} \frac{e^{-\frac{\psi_{th_2}m_i}{\left(a_2-a_1\psi_{th_2}\right)\bar{\rho}_R\lambda_i}-\frac{m_{RP}\rho_D}{\lambda_{RP}\bar{\rho}_R}}}{n_{RP}!n_i!}\left(\frac{\psi_{th_2}n_i}{\left(a_2-a_1\psi_{th_2}\right)\bar{\rho}_R\lambda_i}\right)^{n_i}\left(\frac{\rho_D m_{RP}}{\bar{\rho}_R\lambda_{RP}}\right)^{n_{RP}} \\
& - \sum_{n_i=0}^{m_i-1}\sum_{b_i=0}^{m_{RP}+n_i-1}\binom{m_{RP}+n_i-1}{m_{RP}-1}\left(\frac{\rho_D m_{RP}}{\bar{\rho}_R\lambda_{RP}}\right)^{m_{RP}}\left(\frac{\psi_{th_2}m_i}{\left(a_2-a_1\psi_{th_2}\right)\lambda_i\bar{\rho}_R}\right)^{n_i} \\
& \times \frac{e^{-\frac{\psi_{th_2}\lambda_{RP}m_i+\left(a_2-a_1\psi_{th_2}\right)m_{RP}\lambda_i\rho_D}{\left(a_2-a_1\psi_{th_2}\right)\lambda_i\lambda_{RP}\bar{\rho}_R}}}{b_i!}\left(\frac{\left(a_2-a_1\psi_{th_2}\right)\lambda_i\lambda_{RP}\bar{\rho}_R}{\psi_{th_2}m_i\lambda_{RP}+\left(a_2-a_1\psi_{th_2}\right)m_{RP}\lambda_i\rho_D}\right)^{m_{RP}+n_i-b_i}
\end{aligned} \tag{15}
$$

$$
\begin{aligned}
F_{\Gamma_{R,x_2}}\left(\psi_{th_2}\right) = {} & 1 - \alpha_{SR}\sum_{n_{SR}=0}^{m_{SR}-1}\zeta_{SR}\left(n_{SR}\right)e^{-\frac{\psi_{th_2}\left(\beta_R-\delta_R\right)}{\bar{\rho}_S\left(a_2-a_1\psi_{th_2}\right)}}\sum_{k_{SR}=0}^{n_{SR}}\frac{n_{SR}!}{k_{SR}!}\frac{\left(\psi_{th_2}/\bar{\rho}_S\left(a_2-a_1\psi_{th_2}\right)\right)^{k_{SR}}}{\left(\beta_R-\delta_R\right)^{n_{SR}-k_{SR}+1}} \\
& \times \left(1 - \alpha_{SP}\sum_{n_{SP}=0}^{m_{SP}-1}\zeta_{SP}\left(n_{SP}\right)e^{-\frac{\rho_D\left(\beta_{SP}-\delta_{SP}\right)}{\bar{\rho}_S}}\sum_{k_{SP}=0}^{n_{SP}}\frac{n_{SP}!}{k_{SP}!}\frac{\left(\rho_D/\bar{\rho}_S\right)^{k_{SP}}}{\left(\beta_{SP}-\delta_{SP}\right)^{n_{SP}-k_{SP}+1}}\right) \\
& - \sum_{n_{SP}=0}^{m_{SP}}\zeta_{SP}\left(n_{SP}\right)\sum_{n_{SR}=0}^{m_{SR}-1}\zeta_{SR}\left(n_{SR}\right)\sum_{k_{SR}=0}^{n_{SR}}\sum_{c=0}^{n_{SP}+k_{SR}}\frac{\left(n_{SP}+k_{SR}\right)!n_{SR}!\alpha_{SP}\alpha_{SR}}{k_{SR}!c!\left(\beta_{SR}-\delta_{SR}\right)^{n_{SR}-k_{SR}+1}} \\
& e^{-\left(\frac{\left(\beta_{SP}-\delta_{SP}\right)\rho_D}{\bar{\rho}_S}+\frac{\psi_{th_2}\left(\beta_{SR}-\delta_{SR}\right)}{\left(a_2-a_1\psi_{th_2}\right)\bar{\rho}_S}\right)}\left(\frac{\psi_{th_2}}{\left(a_2-a_1\psi_{th_2}\right)\rho_D}\right)^{k_{SR}}\left(\beta_{SP}-\delta_{SP}+\frac{\psi_{th_2}\left(\beta_{SR}-\delta_{SR}\right)}{\left(a_2-a_1\psi_{th_2}\right)\rho_D}\right)^{c-n_{SP}-k_{SR}-1}
\end{aligned} \tag{16}
$$

$$
\begin{aligned}
OP_{D_1} = {} & 1 - \left(\sum_{k_{SR}=0}^{m_{SR}-1}\zeta_{SR}\left(k_{SR}\right)\sum_{l_{SR}=0}^{k_{SR}}\frac{\alpha_{SR}k_{SR}!\left(\psi_{th_1}/\bar{\rho}_S a_1\right)^{l_{SR}}}{l_{SR}!\left(\beta_R-\delta_R\right)^{k_{SR}-l_{SR}+1}}e^{-\frac{\psi_{th_1}\left(\beta_{SR}-\delta_{SR}\right)}{\bar{\rho}_S a_1}}\right. \\
& \times \left(1 - \sum_{k_{SP}=0}^{m_{SP}-1}\zeta_{SP}\left(k_{SP}\right)\sum_{l_{SP}=0}^{k_{SP}}\frac{k_{SP}!\alpha_{SP}\left(\rho_D/\bar{\rho}_S\right)^{l_{SP}}e^{-\frac{\rho_D\left(\beta_{SP}-\delta_{SP}\right)}{\bar{\rho}_S}}}{l_{SP}!\left(\beta_{SP}-\delta_{SP}\right)^{k_{SP}-l_{SP}+1}}\right) \\
& + \sum_{k_{SR}=0}^{m_{SR}-1}\zeta_{SR}\left(k_{SR}\right)\sum_{k_{SP}=0}^{m_{SP}-1}\zeta_{SP}\left(k_{SP}\right)\sum_{l_{SR}=0}^{k_{SR}}\sum_{l_{SP}=0}^{k_{SP}+l_{SP}}\frac{\alpha_{SP}\alpha_{SR}k_{SR}!\left(k_{SP}+l_{SP}\right)!\left(\rho_D/\bar{\rho}_S\right)^{l_{SP}}}{l_{SR}!l_{SP}!\left(\beta_{SR}-\delta_{SR}\right)^{k_{SR}-l_{SR}+1}} \\
& \times \left(\frac{\psi_{th_1}}{\rho_D a_1}\right)^{l_{SR}}\left(\frac{\psi_{th_1}\left(\beta_R-\delta_R\right)}{\rho_D a_1}+\left(\beta_{SP}-\delta_{SP}\right)\right)^{l_{SP}-k_{SP}-l_{SP}-1}e^{-\left(\frac{\psi_{th_1}\left(\beta_{SR}-\delta_{SR}\right)}{\bar{\rho}_S a_1}+\frac{\left(\beta_{SP}-\delta_{SP}\right)}{\bar{\rho}_S}\right)}\right) \\
& \times \sum_{n_1=0}^{m_1-1}\frac{e^{-\frac{\psi_{th_1}m_1}{a_1\bar{\rho}_R\lambda_1}}}{n_1!}\left(\frac{\psi_{th_1}m_1}{a_1\bar{\rho}_R\lambda_1}\right)^{n_1}\left(1-\sum_{n_{RP}=0}^{m_{RP}-1}\frac{e^{-\frac{m_{RP}\rho_D}{\lambda_{RP}\bar{\rho}_R}}}{n_{RP}!}\left(\frac{\rho_D m_{RP}}{\bar{\rho}_R\lambda_{RP}}\right)^{n_{RP}}\right) + \sum_{n_1=0}^{m_1-1}\sum_{b_1=0}^{m_{RP}+n_1-1}\binom{m_{RP}+n_1-1}{m_{RP}-1}\left(\frac{\rho_D m_{RP}}{\bar{\rho}_R\lambda_{RP}}\right)^{m_{RP}} \\
& \times \frac{\left(\psi_{th_1}m_1/a_1\lambda_1\bar{\rho}_R\right)^{n_1}}{b_1!}\left(\frac{a_1\lambda_1\lambda_{RP}\bar{\rho}_R}{\psi_{th_1}m_1\lambda_{RP}+a_1 m_{RP}\lambda_1\rho_D}\right)^{m_{RP}+n_1-b_1}e^{-\frac{\psi_{th_1}\lambda_{RP}m_1+a_1 m_{RP}\lambda_1\rho_D}{a_1\lambda_1\lambda_{RP}\bar{\rho}_R}}\right)
\end{aligned} \tag{22}
$$

C. DIVERSITY ORDER ANALYSIS

In this paper, we consider the peak interference constraint scenario as [33], where P_D is fixed and only $\bar{P}_j$ becomes large in the high SNR regime.

It is worth noting that the diversity order for D_1, D_2 are defined by

$$d = -\lim_{\bar{\rho} \to \infty} \frac{\log\left(OP_{D_i}^{\infty}(\bar{\rho})\right)}{\log \bar{\rho}} \qquad (23)$$

First, we can write OP_{D_2} as

$$OP_{D_2}^{\infty} = 1 - \left(1 - F_{\Gamma_{R,x_2}}^{\infty}\left(\psi_{th_2}\right)\right)$$
$$\times \left(1 - F_{\Gamma_{D_1,x_2}}^{\infty}\left(\psi_{th_2}\right)\right)\left(1 - F_{\Gamma_{D_2,x_2}}^{\infty}\left(\psi_{th_2}\right)\right) \qquad (24)$$

It is interestingly to find $F_{\Gamma_{R,x_2}}^{\infty}\left(\psi_{th_2}\right)$, $F_{\Gamma_{D_1,x_2}}^{\infty}\left(\psi_{th_2}\right)$ and $F_{\Gamma_{D_2,x_2}}^{\infty}\left(\psi_{th_2}\right)$ which can be expressed in Proposition 1 and 2 as follows.

Proposition 1: The asymptotic expression of $F_{\Gamma_{R,x_2}}^{\infty}\left(\psi_{th_2}\right)$ can be formulated as

$$F_{\Gamma_{R,x_2}}^{\infty}\left(\psi_{th_2}\right)$$
$$= \sum_{k=0}^{m_{SP}-1} \frac{\zeta(k)\,\alpha_{SR}\alpha_{SP}\psi_{th_2}}{(\beta_{SP} - \delta_{SP})^{k+1}\left(a_2 - \psi_{th_2}a_1\right)}$$
$$\times \left(\frac{\gamma\left(k+1, \frac{\rho_D(\beta_{SP}-\delta_{SP})}{\bar{\rho}_S}\right)}{\bar{\rho}_S} + \frac{\Gamma\left(k+2, \frac{\rho_D(\beta_{SP}-\delta_{SP})}{\bar{\rho}_S}\right)}{\rho_D\left(\beta_{SP} - \delta_{SP}\right)}\right) \qquad (25)$$

Proof: See Appendix C.

Proposition 2: The asymptotic expression of $F_{\Gamma_{D_i,x_2}}^{\infty}\left(\psi_{th_2}\right)$ can be formulated by

$$F_{\Gamma_{D_i,x_2}}^{\infty}\left(\psi_{th_2}\right)$$
$$= \frac{\left(\psi_{th_2}m_i/\lambda_i\left(a_2 - \psi_{th_2}a_1\right)\right)^{m_i}}{\Gamma(m_i+1)\,\Gamma(m_{RP})}$$
$$\times \left(\frac{\gamma\left(m_{RP}, \frac{m_{RP}\rho_D}{\lambda_{RP}\bar{\rho}_R}\right)}{(\bar{\rho}_R)^{m_i}} + \frac{\Gamma\left(m_{RP}+m_i, \frac{m_{RP}\rho_D}{\lambda_{RP}\bar{\rho}_R}\right)}{(\rho_D m_{RP}/\lambda_{RP})^{m_i}}\right). \qquad (26)$$

Proof: See Appendix D.

Next, the asymptotic expression of OP for user D_1 and it is given by

$$OP_{D_1}^{\infty} = 1 - \left(1 - F_{\Gamma_{R,x_1}}^{\infty}\left(\psi_{th_2}\right)\right)$$
$$\times \left(1 - F_{\Gamma_{D_1,x_1}}^{\infty}\left(\psi_{th_2}\right).\right) \qquad (27)$$

It is noted that (27) can be achieved based on the following computations. Similarly, $F_{\Gamma_{R,x_1}}^{\infty}\left(\psi_{th_2}\right)$ and $F_{\Gamma_{D_1,x_1}}^{\infty}\left(\psi_{th_2}\right)$ are given as respectively

$$F_{\Gamma_{R,x_2}}^{\infty}\left(\psi_{th_2}\right)$$
$$= \sum_{k=0}^{m_{SP}-1} \frac{\zeta(k)\,\alpha_{SR}\alpha_{SP}\psi_{th_1}}{(\beta_{SP} - \delta_{SP})^{k+1}\,a_1}$$
$$\times \left(\frac{\gamma\left(k+1, \frac{\rho_D(\beta_{SP}-\delta_{SP})}{\bar{\rho}_S}\right)}{\bar{\rho}_S} + \frac{\Gamma\left(k+2, \frac{\rho_D(\beta_{SP}-\delta_{SP})}{\bar{\rho}_S}\right)}{\rho_D\left(\beta_{SP} - \delta_{SP}\right)}\right), \qquad (28)$$

and

$$F_{\Gamma_{D_1,x_1}}^{\infty}\left(\psi_{th_2}\right)$$
$$= \frac{\left(\psi_{th_2}m_1/\lambda_1 a_1\right)^{m_1}}{\Gamma(m_1+1)\,\Gamma(m_{RP})}$$
$$\times \left(\frac{\gamma\left(m_{RP}, \frac{m_{RP}\rho_D}{\lambda_{RP}\bar{\rho}_R}\right)}{(\bar{\rho}_R)^{m_1}} + \frac{\Gamma\left(m_{RP}+m_1, \frac{m_{RP}\rho_D}{\lambda_{RP}\bar{\rho}_R}\right)}{(\rho_D m_{RP}/\lambda_{RP})^{m_1}}\right). \qquad (29)$$

Remark 2: We can infer from (24) and (27) that the secondary network of such CR-NHST exhibits different performance of two users which depends on transmit SNRThe diversity order of OP_{D_i} is zero in transmit power at some nodes. It can be concluded that the diversity order of OP_{D_i} is zero in high SNR. This is predicted that outage performance is flat curves at high region of transmit SNR at the source.

D. THROUGHPUT PERFORMANCE

The overall throughput is an another performance metric for such systems, which can be evaluated with the help of outage probabilities. In delay-limited mode, at fixed target rates R_1, R_2, the throughput can be achieved. As a result, the overall throughput can be formulated as

$$T_{total} = \left(1 - OP_{D_1}\right)R_1 + \left(1 - OP_{D_2}\right)R_2. \qquad (30)$$

E. ERGODIC CAPACITY ANALYSIS

By using definition, the ergodic rate of x_1 is given by

$$C_{x_1} = \frac{1}{2}E\left[\log_2\left(1 + Z_1\right)\right]$$
$$= \frac{1}{2\ln 2}\int_0^{\infty} \frac{1 - F_{Z_1}(x)}{1 + x}dx, \qquad (31)$$

where $Z_1 = \min\left(\Gamma_{R,x_1}, \Gamma_{D_1,x_1}\right)$. Then, the CDF of Z_1 is expressed as

$$F_{Z_1}(x) = \Pr\left(\min\left(\Gamma_{R,x_1}, \Gamma_{D_1,x_1}\right) < x\right)$$
$$= 1 - \left(1 - F_{\Gamma_{R,x_1}}(x)\right)\left(1 - F_{\Gamma_{D_1,x_1}}(x)\right) \qquad (32)$$

Based on (20) and (21), we obtain the PDF of Z_1. Unfortunately, it is difficult to obtain a closed-form expression from (31) as [35].

Next, the ergodic rate of x_2 is given by

$$
\begin{aligned}
C_{x_2} &= \frac{1}{2} E \left[\log_2 \left(1 + Z_2 \right) \right] \\
&= \frac{1}{2 \ln 2} \int_0^\infty \frac{1 - F_{Z_2}(y)}{1 + y} dx
\end{aligned}
\tag{33}
$$

where $Z_2 = \min \left(\Gamma_{R,x_2}, \Gamma_{D_2,x_2}, \Gamma_{D_1,x_2} \right)$. Furthermore, the CDF of Z_2 is obtained as

$$
\begin{aligned}
&F_{Z_2}(y) \\
&= \Pr \left(\min \left(\Gamma_{R,x_2}, \Gamma_{D_2,x_2}, \Gamma_{D_1,x_2} \right) < y \right) \\
&= 1 - \left(1 - F_{\Gamma_{R,x_2}}(y) \right) \left(1 - F_{\Gamma_{D_2,x_2}}(y) \right) \left(1 - F_{\Gamma_{D_1,x_2}}(y) \right)
\end{aligned}
\tag{34}
$$

With the help (15) and (16), the PDF of Z_2 could be computed. To the best of authors' knowledge, (33) does not have a closed-form solution [35].

F. ENERGY EFFICIENCY
To further evaluate the performance of the considered systems, energy efficiency (EE) could be examined as an important criteria, which is defined as the bits of information reliably transferred the receivers per unit consumed energy at the transmitters [36]

$$
\eta_{EE} = \frac{\text{Total data rate}}{\text{Total energy consumption}}.
\tag{35}
$$

Based on the throughput analysis in (30), the energy efficiency of the considered systems is given by

$$
\eta_{EE} = \frac{2 T_{total}}{T \left(P_S + P_R \right)},
\tag{36}
$$

where T denotes the transmission time for the entire communication process.

IV. EXTENSION TO SCENARIO OF MULTIPLE USERS
We continue to evaluate how multiple users make degraded performance of specific group of users in the context of NOMA. Ideally, two-user scenario is considered in the previous section which motivate us to further examine the groups containing N users, i.e. denoting them as $(D_1, D_2, \ldots, D_{N-1}, D_N)$. In such circumstance, the source S intends to proceed the superimposed signals $\sum_{n=1}^{N} \sqrt{a_n P_S} x_n + n_R$ to R. For signal processing for user D_N, x_n is targeted to it, and this user is allocated the percentage of total power, i.e. a_n with the constraint $a_1 > a_2 > \ldots > a_N$ and $\sum_{n=1}^{N} a_n = 1$. In term of multiple users in groups of NOMA system, it is usually assumed the channel ordering could be $h_1 < h_2 < \ldots < h_{N-1} < h_N$.

In practical scenarios, a multi-user multi-relay architecture for NOMA aided CR-NHST has been explored. However, by grouping pair of users, such system can satisfy particular requirements of paired users.

TABLE 3. Channel parameters.

Shadowing	b	m	Ω
Average shadowing (AS)	0.251	5	0.279
Heavy shadowing (HS)	0.063	1	0.0007

In the first phase, the received signal at R can be formulated by

$$
y_{RN} = h_{SR} \sum_{n=1}^{N} \sqrt{P_S a_n} x_n + n_R.
\tag{37}
$$

Further, after receiving the mixture signals, R needs assistance of the SIC in the context of NOMA [39]. In particular, R detects the signal x_1 and considers other signal($q = 2, 3, \ldots, N$) as noise. In the next stage, R decodes the signal x_2 and the noise in this case could be $x_q, (q = 3, 4, \ldots, N)$. As expectation in the last step, R decodes the signal x_N. Therefore, the SINR of detecting x_q at R is computed by

$$
\Gamma_{R,q} = \frac{|h_{SR}|^2 P_S a_q}{|h_{SR}|^2 P_S \sum_{p=i+1}^{N} a_p + \sigma_R^2}.
\tag{38}
$$

Finally, the SINR at R detects the signal x_N is given as

$$
\Gamma_{R,N} = \frac{|h_{SR}|^2 P_S a_N}{\sigma_R^2}
\tag{39}
$$

During the second phase, R forwards the detected signal to $D_m (m \in (1, 2, \ldots, N))$. The signal at D_m is given as

$$
y_m = h_m \sum_{n=1}^{N} \sqrt{P_R a_p} x_p + n_{D_m}.
\tag{40}
$$

Similar to R, D_m executes the SIC to decode the signal $x_q (1 \leqslant q \leqslant m \leqslant N)$. The SINR can be written as

$$
\Gamma_{m,q} = \frac{|h_m|^2 P_R a_q}{|h_m|^2 P_R \sum_{p=i+1}^{N} a_p + \sigma_m^2}.
\tag{41}
$$

The SNR of D_N to detect the own signal is given as

$$
\Gamma_N = \frac{|h_N|^2 P_R a_N}{\sigma_m^2}.
\tag{42}
$$

Finally, the achievable rate of the messages devoted to $D_q (1 \leqslant q \leqslant m \leqslant N)$ and D_N are accordingly expressed by [40]

$$
R_q = \frac{1}{2} \log_2 \left[1 + \min \left(\Gamma_{R,q}, \Gamma_{m,q} \right) \right],
\tag{43}
$$

$$
R_N = \frac{1}{2} \log_2 \left[1 + \min \left(\Gamma_{R,N}, \Gamma_N \right) \right].
\tag{44}
$$

V. NUMERICAL RESULTS
In this section, to verify mathematical analysis, it is necessary to simulate and illustrate for proposed assisted CR-NOMA scheme. Here, the shadowing scenarios of the satellite links h_{Sk}, including the average shadowing (AS) and the heavy shadowing (HS) being given in Table 3 [1], [37].
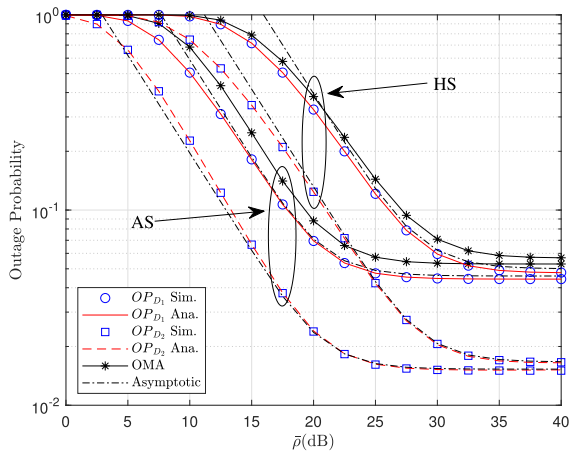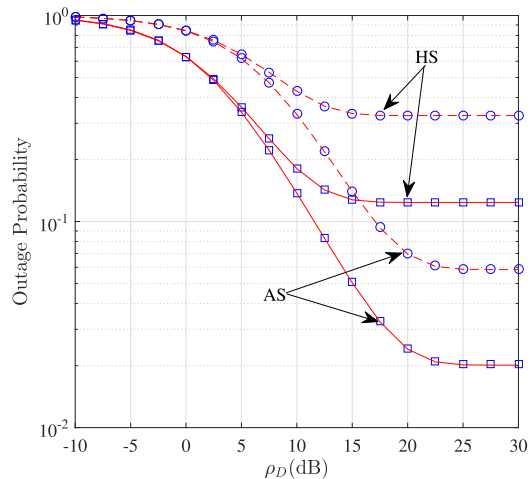
FIGURE 2. The outage probability versus $\bar{\rho}$ with different values of the satellite link, where $m_{RP} = m_1 = m_2 = 2$, $\rho_D = 20$dB.

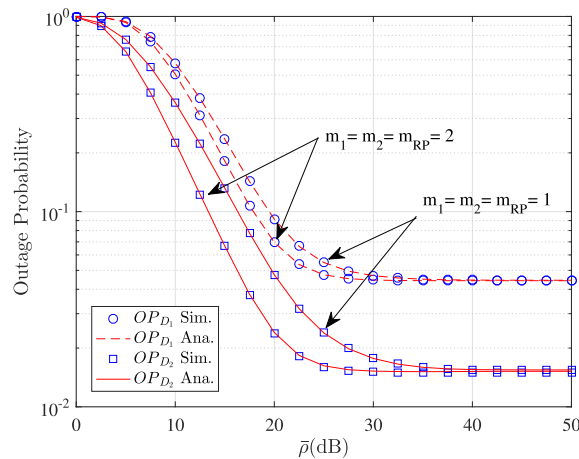**FIGURE 3.** The OP versus ρ_D, with different values of the satellite link, where $\bar{\rho} = 20$dB, $m_{RP} = m_1 = m_2 = 2$.

FIGURE 4. The OP versus ρ_D, with different values of $m_{RP} = m_1 = m_2$, where $\bar{\rho} = \rho_D = 20$ dB and the satellite link set HS case.

We set power allocation factors $a_1 = 0.2$, $a_2 = 0.8$, $\bar{\rho} = \bar{\rho}_S = \bar{\rho}_R$, the target rates $R_1 = R_2 = 0.5$ bit per channel use (BPCU) except for specific cases, the channel gains $\lambda_{SP} = 0.01$, $\lambda_1 = 2$, $\lambda_2 = 1$ and $m_{RP} = m_1 = m_2$. Moreover, case of $m_{RP} = m_1 = m_2 = 1$ is equivalent with the Rayleigh fading channel model. In these following figures, Monte-Carlo simulations are performed to validate the analytical results.

In Fig. 2, we plot the OP curves for the secondary network of CR-NHST (with two sets of channel, i.e. HS and AS) under impact of SNR at the satellite. In particular, it can be seen good matching between the analytical and simulated OP curves. Such observation definitely confirm how exactly our expressions presented in in Sections III. We can see that the OP performance can be improved if we increase SNR at the satellite approach 15 dB. It is very important to point out that asymptotic lines are matched with exact curves at high SNR region. This result is definitely confirmed exactness of our derived expressions. But, if we continue to increase SNR, the OP curves still remain unchanged. As a result, the expression of diversity order in previous section is verified. For comparison, we have also plotted the OP curves for benchmark of OMA transmission. The case of AS in such CR-NHST shows the best performance among these cases. It shows that OMA is worst case. Similar trends of OP curves can be seen in Fig. 3. When we increase ρ_D, which means the transmit power at the satellite increases, OP performance can be enhanced.

Fig. 4 plots the OP curves for the secondary network of considered system under Nakagami-*m* faded terrestrial links. Herein, it can be concluded that $m_1 = m_2 = m_{RP} = 2$ exhibit the best performance. We can see that the analytical OP curves for two users converge to floor value when the transmit SNR is higher than 30 dB. The performance gap exists among two users due to different power allocation factors and condition of SIC. In Fig. 5, we investigate the target rates which make influence on OP curves for two NOMA users. As definition of OP, the target rates limit performance

of OP in such network. For such, the lower required target rates contribute to better OP performance for two users.

We can study the impacts of power allocation factors a_1, a_2 on the OP of two users in Fig. 6. When we increase a_1, the SINR to detect user D_1's signal increases and hence the value of OP for user D_1 becomes smaller. While the OP performance of user D_2 would be worse as increasing a_1. The main reason is that SINR is computed based many parameters including a_1, a_2.

In Fig. 7, depending on the OP performance, the throughput of considered system increases significantly as the transmit SNR at the satellite increases from 0 dB to 40 dB. It is clearly that there is existence of ceiling value of such throughput at high region of SNR.

Interestingly, in Fig. 8, we can find optimal throughput in HS and AS configuration for proper target rates $R_1 = R_2$. The superiority of this system with AS scheme still remain in this experiment.

Due to difference among expressions of SINR for two users, we show different ergodic capacity performance,
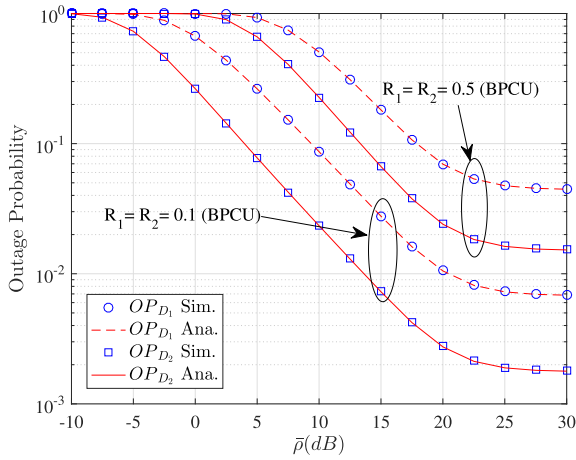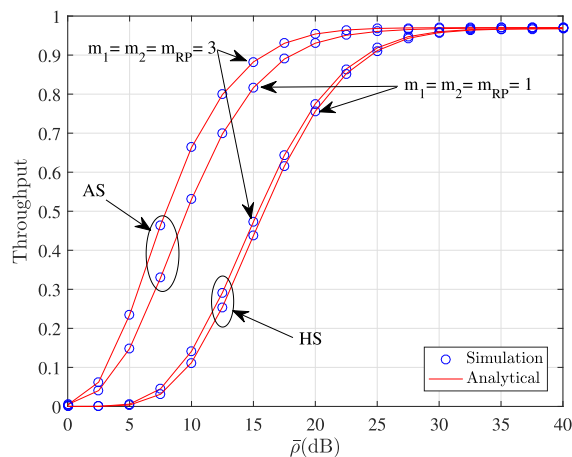
FIGURE 5. The outage probability versus $\bar{\rho}$, with different values of $R_1 = R_2$, where $\rho_D = 20$dB, $m_{RP} = m_1 = m_2 = 2$ and the satellite link is set AS case.
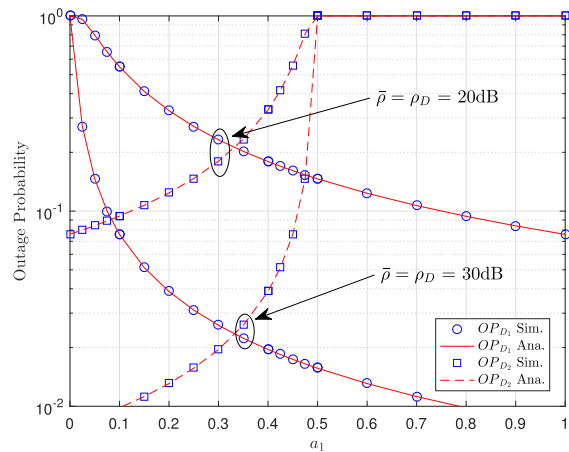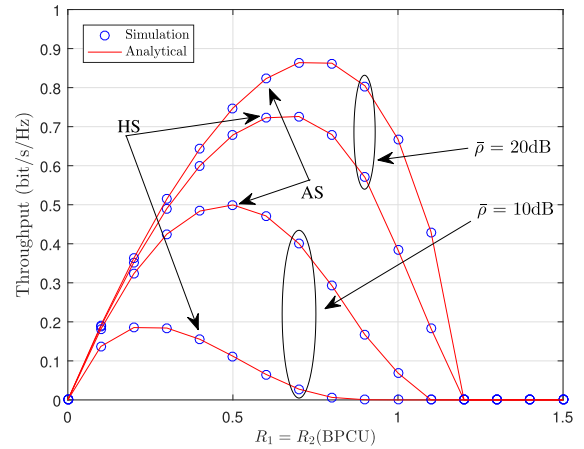

FIGURE 6. The outage probability versus a_1, with different values of $\bar{\rho} = \rho_D$, where $m_{RP} = m_1 = m_2 = 2$ and the satellite link is set HS case.
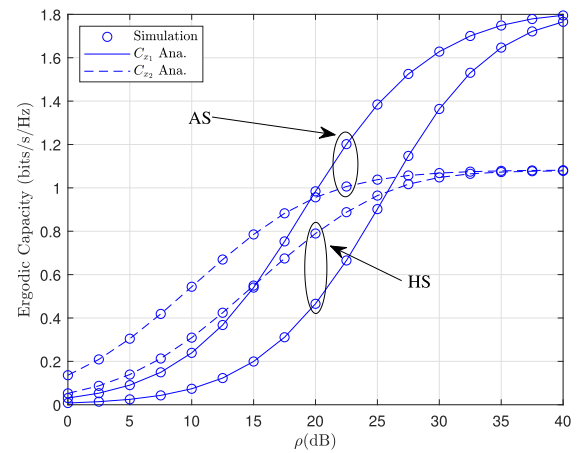

FIGURE 7. The throughput versus $\bar{\rho}$ where $\rho_D = 20$dB.

FIGURE 8. The throughput versus $R_1 = R_2$ where $\rho_D = 10$dB and $m_{RP} = m_1 = m_2 = 1$.

FIGURE 9. The ergodic capacity versus ρ(dB) where $\rho_D = 20$dB and $m_{RP} = m_1 = m_2 = 1$.

FIGURE 10. The energy efficiency versus ρ(dB) where $\rho_D = 20$dB and $m_{RP} = m_1 = m_2 = 1$.
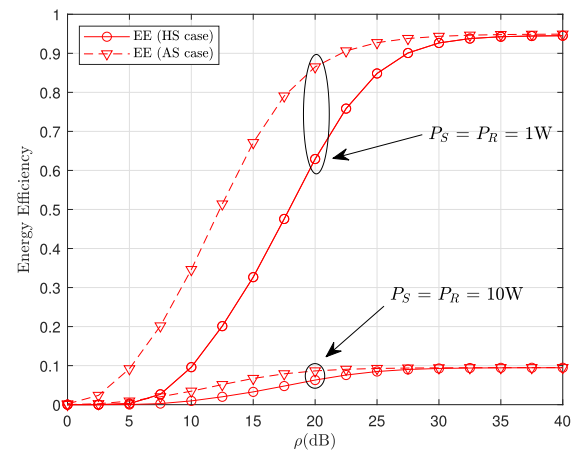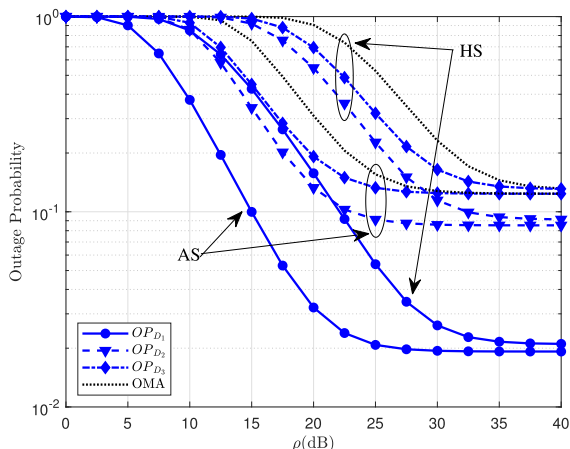
as shown in Fig. 9. It can be seen intuitively that, the ergodic capacity of the first user is better than that of the second user. In meantime, we also examine EE for two configurations (HS and AS) for our considered system, shown in Fig. 10. At high SNR, EE curves also meet their ceiling values. The main reason it that the corresponding throughput is limited at high SNR region.

FIGURE 11. Multiple users case: The outage probability versus $\bar{\rho}$ with different values of the satellite link, where $m_{RP} = m_1 = m_2 = 2$, $\rho_D = 20$dB, $a_1 = 0.5$, $a_2 = 0.3$, $a_3 = 0.2$, $R_1 = 0.3$, $R_1 = 0.5$ and $R_3 = 1$.

It is more challenging when we consider multiple users scenario, shown in Fig. 11. In particular, user D_3 has power allocation factor $a_3 = 0.2$ and its performance is worse than the others. This circumstance can be explained that more interference and less power are joint happened in all users in a specific group and such issue becomes crucial if the number of users is greater than 2.

VI. CONCLUSION

In this study, we have investigated the system performance of the CR-NHST system relying on NOMA in terms of outage probability, ergodic capacity, energy efficiency and throughput. In particular, we have derived the closed-form expressions of outage probability, defined expression of ergodic capacity to show how different performance of the two users in the secondary network over some sets of channels. These derived expressions were validated by numerical results, and the outage events of two users were compared with OMA case. The asymptotic computation of outage probability and diversity order are also provided to show more insights related to performance analysis. Moreover, the numerical results showed that the proper selection of power allocation factors and transmit SNR at the satellite can guarantee the performance fairness for both users.

As most of papers in literature, it is assumed the knowledge of perfect channel state information (CSI) in such CR-NHST to facilitate the user selection process. Although the CSI for user selection may be outdated due to various reasons such as feedback delay, mobility, etc. Further, with dense frequency reuse in wireless networks, the HSTRN is prone to co-channel interference (CCI). These challenges need be addressed in extra effort in our future work.

APPENDIX A
We recall expression of $F_{\Gamma_{D_1,x_2}} \left(\psi_{th_2} \right)$ as below

$$F_{\Gamma_{D_1,x_2}} \left(\psi_{th_2} \right)$$
$$= 1 - \Pr \left(\frac{P_R a_2 |h_1|^2}{P_R a_1 |h_1|^2 + \sigma_1^2} > \psi_{th_2} \right)$$

$$= 1 - \underbrace{\Pr \left(\frac{\bar{\rho}_R a_2 |h_1|^2}{\bar{\rho}_R a_1 |h_1|^2 + 1} > \psi_{th_2}, |h_{RP}|^2 < \frac{\rho_D}{\bar{\rho}_R} \right)}_{A_1}$$

$$- \underbrace{\Pr \left(\frac{\rho_D a_2 |h_1|^2}{\rho_D a_1 |h_1|^2 + |h_{RP}|^2} > \psi_{th_2}, |h_{RP}|^2 > \frac{\rho_D}{\bar{\rho}_R} \right)}_{A_2}, \quad (45)$$

in which $\bar{\rho}_R = \frac{\bar{P}_R}{\sigma^2}, \sigma^2 = \sigma_R^2 = \sigma_1^2 = \sigma_2^2$ and $\rho_D = \frac{P_D}{\sigma^2}$. Then, we can rewrite A_1 as

First, A_1 is expressed by

$$A_1 = \Pr \left(|h_1|^2 > \frac{\psi_{th_2}}{\bar{\rho}_R \left(a_2 - a_1 \psi_{th_2} \right)}, |h_{RP}|^2 < \frac{\rho_D}{\bar{\rho}_S} \right)$$

$$= \int_{\frac{\psi_{th_2}}{\bar{\rho}_R \left(a_2 - a_1 \psi_{th_2} \right)}}^{\infty} f_{|h_1|^2} (x) \int_0^{\frac{\rho_D}{\bar{\rho}_S}} f_{|h_{RP}|^2} (y) dy dx. \quad (46)$$

Then, A_1 is rewritten as

$$A_1 = \sum_{n_1=0}^{m_1-1} \frac{e^{-\frac{\psi_{th_2} m_1}{\left(a_2 - a_1 \psi_{th_2} \right) \bar{\rho}_R \lambda_1}}}{n_1!} \left(\frac{\psi_{th_2} n_1}{\left(a_2 - a_1 \psi_{th_2} \right) \bar{\rho}_R \lambda_2} \right)^{n_1}$$

$$- \sum_{n_1=0}^{m_1-1} \sum_{n_{RP}=0}^{m_{RP}-1} \frac{e^{-\frac{\psi_{th_2} m_1}{\left(a_2 - a_1 \psi_{th_2} \right) \bar{\rho}_R \lambda_1} - \frac{m_{RP} \rho_D}{\lambda_{RP} \bar{\rho}_R}}}{n_{RP}! n_1!}$$

$$\times \left(\frac{\psi_{th_2} n_1}{\left(a_2 - a_1 \psi_{th_2} \right) \bar{\rho}_R \lambda_1} \right)^{n_1} \left(\frac{\rho_D m_{RP}}{\bar{\rho}_R \lambda_{RP}} \right)^{n_{RP}}. \quad (47)$$

Secondly, it can be obtained A_2 as

$$A_2 = \Pr \left(|h_1|^2 > \frac{\psi_{th_2} |h_{RP}|^2}{\rho_D a_2 - \psi_{th_2} \rho_D a_1}, |h_{RP}|^2 > \frac{\rho_D}{\bar{\rho}_R} \right)$$

$$= \int_{\frac{\rho_D}{\bar{\rho}_R}}^{\infty} f_{|h_{RP}|^2} (y) \int_{\frac{\psi_{th_2} y}{\rho_D a_2 - \psi_{th_2} \rho_D a_1}}^{\infty} f_{|h_1|^2} (x) dx dy. \quad (48)$$

Then, A_2 is rewritten as

$$A_2 = \sum_{n_1=0}^{m_1-1} \frac{(m_{RP}/\lambda_{RP})^{m_{RP}}}{n_1! \Gamma (m_{RP})} \left(\frac{\psi_{th_2} m_1}{\left(a_2 - a_1 \psi_{th_2} \right) \lambda_1 \rho_D} \right)^{n_1}$$

$$\times \int_{\frac{\rho_D}{\bar{\rho}_R}}^{\infty} y^{m_{RP}+n_1-1} e^{-\left(\frac{\psi_{th_2} m_1}{\left(a_2 - a_1 \psi_{th_2} \right) \lambda_1 \rho_D} + \frac{m_{RP}}{\lambda_{RP}} \right) y} dy. \quad (49)$$

Finally, we can achieve A_1 as

A_2

$$
= \sum_{n_1=0}^{m_1-1} \sum_{b_1=0}^{m_{RP}+n_1-1} \binom{m_{RP}+n_1-1}{m_{RP}-1} \left(\frac{\rho_D m_{RP}}{\bar{\rho}_R \lambda_{RP}} \right)^{m_{RP}}
$$

$$
\times \left(\frac{\psi_{th_2} m_1}{(a_2 - a_1 \psi_{th_2}) \lambda_1 \bar{\rho}_R} \right)^{n_1} \frac{e^{-\frac{\psi_{th_2} \lambda_{RP} m_1 + (a_2-a_1\psi_{th_2}) m_{RP}\lambda_1 \rho_D}{(a_2-a_1\psi_{th_2})\lambda_1 \lambda_{RP}\bar{\rho}_R}}}{b_1!}
$$

$$
\times \left(\frac{(a_2 - a_1 \psi_{th_2}) \lambda_1 \lambda_{RP} \bar{\rho}_R}{\psi_{th_2} m_1 \lambda_{RP} + (a_2 - a_1 \psi_{th_2}) m_{RP} \lambda_1 \rho_D} \right)^{m_{RP}+n_1-b_1}.
$$

$$(50)$$

Similarly, we easy obtain $F_{\Gamma_{D_2,x_2}}(\psi_{th_2})$. This completes the proof of lemma 1.

APPENDIX B

First, $F_{\Gamma_{R,x_2}}(\psi_{th_2})$ can be formulated by

$$
F_{\Gamma_{R,x_2}}(\psi_{th_2})
$$

$$
= 1 - \Pr \left(\frac{P_S a_2 |h_{SR}|^2}{P_S a_1 |h_{SR}|^2 + \sigma_R^2} > \psi_{th_2} \right)
$$

$$
= 1 - \underbrace{\Pr \left(\frac{\bar{\rho}_S a_2 |h_{SR}|^2}{\bar{\rho}_S a_1 |h_{SR}|^2 + 1} > \psi_{th_2}, |h_{SP}|^2 < \frac{\rho_D}{\bar{\rho}_S} \right)}_{B_1}
$$

$$
- \underbrace{\Pr \left(\frac{\rho_D a_2 |h_{SR}|^2}{\rho_D a_1 |h_{SR}|^2 + |h_{SP}|^2} > \psi_{th_2}, |h_{SP}|^2 > \frac{\rho_D}{\bar{\rho}_S} \right)}_{B_2},
$$

$$(51)$$

where $\bar{\rho}_S = \frac{\bar{P}_S}{N_0}$ There are two components can be further computed in the closed-form expressions. We can express B_1 as below

$$
B_1 = \int_0^{\frac{\rho_D}{\bar{\rho}_S}} f_{|h_{SP}|^2}(x) \int_{\frac{\psi_{th_2}}{\bar{\rho}_S (a_2 - a_1 \psi_{th_2})}}^{\infty} f_{|h_{SR}|^2}(y) \, dx \, dy. \quad (52)
$$

Then, it can be obtained B_1 as

$$
B_1 = \alpha_{SR} \sum_{n_{SR}=0}^{m_{SR}-1} \zeta_{SR}(n_{SR}) e^{-\frac{\psi_{th_2}(\beta_{SR}-\delta_{SR})}{\bar{\rho}_S(a_2-a_1\psi_{th_2})}}
$$

$$
\times \sum_{k_{SR}=0}^{n_{SR}} \frac{n_{SR}!}{k_{SR}!} \frac{(\psi_{th_2}/\bar{\rho}_S (a_2 - a_1 \psi_{th_2}))^{k_{SR}}}{(\beta_{SR} - \delta_{SR})^{n_{SR}-k_{SR}+1}}
$$

$$
\times \left(1 - \alpha_{SP} \sum_{n_{SP}=0}^{m_{SP}-1} \zeta_{SP}(n_{SP}) e^{-\frac{\rho_D(\beta_{SP}-\delta_{SP})}{\bar{\rho}_S}} \right.
$$

$$
\left. \times \sum_{k_{SP}=0}^{n_{SP}} \frac{n_{SP}! (\rho_D/\bar{\rho}_S)^{k_{SP}}}{k_{SP}! (\beta_{SP} - \delta_{SP})^{n_{SP}-k_{SP}+1}} \right). \quad (53)
$$

Similarly, we can obtain B_2 as below

$$
B_2 = \sum_{n_{SP}=0}^{m_{SP}} \zeta_{SP}(n_{SP}) \sum_{n_{SR}=0}^{m_{SR}-1} \zeta_{SR}(n_{SR})
$$

$$
\times \sum_{k_{SR}=0}^{n_{SR}} \sum_{c=0}^{n_{SP}+k_{SR}} \frac{(n_{SP}+k_{SR})! n_{SR}! \alpha_{SP} \alpha_{SR}}{k_{SR}! c! (\beta_{SR} - \delta_{SR})^{n_{SR}-k_{SR}+1}}
$$

$$
e^{-\left(\frac{(\beta_{SP}-\delta_{SP})\rho_D}{\bar{\rho}_S} + \frac{\psi_{th_2}(\beta_{SR}-\delta_{SR})}{(a_2-a_1\psi_{th_2})\bar{\rho}_S} \right)} \left(\frac{\psi_{th_2}}{(a_2 - a_1 \psi_{th_2}) \rho_D} \right)^{k_{SR}}
$$

$$
\times \left(\beta_{SP} - \delta_{SP} + \frac{\psi_{th_2}(\beta_{SR}-\delta_{SR})}{(a_2-a_1\psi_{th_2})\rho_D} \right)^{c-n_{SP}-k_{SR}-1}. \quad (54)
$$

This completes the proof of lemma 2.

APPENDIX C

By using (1), the asymptotic of $F_{\rho_S|h_R|^2}^{\infty}(x)$ for peak interference constraint can be obtained as

$$
F_{\rho_S|h_{SR}|^2}^{\infty}(x) = \underbrace{\int_0^{\frac{\rho_D}{\bar{\rho}_S}} F_{\bar{\rho}_S|h_{SR}|^2}^{\infty}(x) f_{|h_{SP}|^2}(y) \, dy}_{Q_1}
$$

$$
+ \underbrace{\int_{\frac{\rho_D}{\bar{\rho}_S}}^{\infty} F_{\bar{\rho}_S|h_{SR}|^2}^{\infty}\left(\frac{xy\bar{\rho}_S}{\rho_D} \right) f_{|h_{SP}|^2}(y) \, dy}_{Q_2}. \quad (55)
$$

Further, at high SNR, we can rewrite $F_{\bar{\rho}_S|h_{SR}|^2}^{\infty}(x)$ as

$$
F_{\bar{\rho}_S|h_{SR}|^2}^{\infty}(x) = \frac{\alpha_{SR} x}{\bar{\rho}_S}. \quad (56)
$$

Furthermore, based on [41, Eq. 3.351.1, Eq. 3.351.2], and (10). Q_1 and Q_2 are obtained as respectively

$$
Q_1 = \sum_{k=0}^{m_{SP}-1} \frac{\zeta(k) \alpha_{SR} \alpha_{SP} x}{\bar{\rho}_S (\beta_{SP} - \delta_{SP})^{k+1}}
$$

$$
\times \gamma \left(k+1, \frac{\rho_D (\beta_{SP} - \delta_{SP})}{\bar{\rho}_S} \right), \quad (57)
$$

$$
Q_2 = \sum_{k=0}^{m_{SP}-1} \frac{\zeta(k) \alpha_{SR} \alpha_{SP} x}{\rho_D (\beta_{SP} - \delta_{SP})^{k+2}}
$$

$$
\times \Gamma \left(k+2, \frac{\rho_D (\beta_{SP} - \delta_{SP})}{\bar{\rho}_S} \right). \quad (58)
$$

Then, substituting (57) and (58) into (55), we have

$$
\begin{aligned}
F_{\rho_S|h_{SR}|^2}^{\infty}(x) \\
= \sum_{k=0}^{m_{SP}-1} \frac{\zeta(k)\,\alpha_{SR}\alpha_{SP}x}{\bar{\rho}_S\,(\beta_{SP}-\delta_{SP})^{k+1}} \\
\times \left(\frac{\gamma\left(k+1, \frac{\rho_D(\beta_{SP}-\delta_{SP})}{\bar{\rho}_S}\right)}{\bar{\rho}_S} + \frac{\Gamma\left(k+2, \frac{\rho_D(\beta_{SP}-\delta_{SP})}{\bar{\rho}_S}\right)}{\rho_D\,(\beta_{SP}-\delta_{SP})} \right).
\end{aligned}
\tag{59}
$$

Finally, with the help (3) and performing necessary manipulations. This proof is completed.

APPENDIX D

By using (1), the asymptotic of $F_{P_S|h_R|^2}^{\infty}(x)$ for peak interference constraint can be obtained as

$$
F_{\rho_R|h_i|^2}^{\infty}(x) = \underbrace{\int_0^{\frac{\rho_D}{\bar{\rho}_R}} F_{|h_i|^2}^{\infty}\left(\frac{x}{\bar{\rho}_R}\right) f_{|h_{RP}|^2}(y)\,dy}_{\bar{Q}_1}
$$
$$
+ \underbrace{\int_{\frac{\rho_D}{\bar{\rho}_R}}^{\infty} F_{|h_i|^2}^{\infty}\left(\frac{xy}{\rho_D}\right) f_{|h_{RP}|^2}(y)\,dy}_{\bar{Q}_2}.
\tag{60}
$$

$$
\gamma\left(m_i, \frac{m_i x}{\lambda_i}\right) \overset{x\to 0}{\approx} \frac{1}{m_i}\left(\frac{m_i x}{\lambda_i}\right)^{m_i}.
\tag{61}
$$

Similarly, we have similar expressions as below. Firstly, the asymptotic of $F_{|h_i|^2}$ can be written as

$$
F_{|h_i|^2}^{\infty}(x) = \frac{1}{\Gamma(m_i+1)}\left(\frac{m_i x}{\lambda_i}\right)^{m_i}.
\tag{62}
$$

Then, $\bar{Q}_1$ and $\bar{Q}_2$ are given respectively by

$$
\bar{Q}_1 = \frac{\gamma\left(m_{RP}, \frac{m_{RP}\rho_D}{\lambda_{RP}\bar{\rho}_R}\right)}{\Gamma(m_i+1)\,\Gamma(m_{RP})}\left(\frac{m_i}{\lambda_i\bar{\rho}_R}x\right)^{m_i},
\tag{63}
$$

$$
\bar{Q}_2 = \frac{\Gamma\left(m_{RP}+m_i, \frac{m_{RP}\rho_D}{\lambda_{RP}\bar{\rho}_R}\right)}{\Gamma(m_i+1)\,\Gamma(m_{RP})}\left(\frac{\lambda_{RP}}{m_{RP}}\right)^{m_i}\left(\frac{m_i x}{\lambda_i\rho_D}\right)^{m_i}.
\tag{64}
$$

Next, we have

$$
\begin{aligned}
F_{\rho_R|h_i|^2}^{\infty}(x) \\
= \frac{1}{\Gamma(m_i+1)\,\Gamma(m_{RP})}\left(\frac{m_i x}{\lambda_i}\right)^{m_i} \\
\times \left(\frac{\gamma\left(m_{RP}, \frac{m_{RP}\rho_D}{\lambda_{RP}\bar{\rho}_R}\right)}{(\bar{\rho}_R)^{m_i}} + \frac{\Gamma\left(m_{RP}+m_i, \frac{m_{RP}\rho_D}{\lambda_{RP}\bar{\rho}_R}\right)}{(\rho_D m_{RP}/\lambda_{RP})^{m_i}} \right).
\end{aligned}
\tag{65}
$$

This completes the proof.

REFERENCES

[1] P. K. Upadhyay and P. K. Sharma, "Max-max user-relay selection scheme in multiuser and multirelay hybrid satellite-terrestrial relay systems," *IEEE Commun. Lett.*, vol. 20, no. 2, pp. 268–271, Feb. 2016.

[2] W. Lu, K. An, and T. Liang, "Robust beamforming design for sum secrecy rate maximization in multibeam satellite systems," *IEEE Trans. Aerosp. Electron. Syst.*, vol. 55, no. 3, pp. 1568–1572, Jun. 2019.

[3] V. Bankey and P. K. Upadhyay, "Average symbol error probability of interference-limited multiuser hybrid satellite-terrestrial relay networks with outdated channel state information," in *Proc. IEEE Region Conf. (TENCON)*, Kochi, India, Oct. 2019, pp. 846–851.

[4] M. K. Arti and V. Jain, "Relay selection-based hybrid satellite-terrestrial communication systems," *IET Commun.*, vol. 11, no. 17, pp. 2566–2574, Nov. 2017.

[5] X. Liang, J. Jiao, S. Wu, and Q. Zhang, "Outage analysis of multirelay multiuser hybrid satellite-terrestrial millimeter-wave networks," *IEEE Wireless Commun. Lett.*, vol. 7, no. 6, pp. 1046–1049, Dec. 2018.

[6] V. Bankey, P. K. Upadhyay, D. B. Da Costa, P. S. Bithas, A. G. Kanatas, and U. S. Dias, "Performance analysis of multi-antenna multiuser hybrid satellite-terrestrial relay systems for mobile services delivery," *IEEE Access*, vol. 6, pp. 24729–24745, 2018.

[7] K. Guo, K. An, B. Zhang, Y. Huang, and G. Zheng, "Outage analysis of cognitive hybrid satellite-terrestrial networks with hardware impairments and multi-primary users," *IEEE Wireless Commun. Lett.*, vol. 7, no. 5, pp. 816–819, Oct. 2018.

[8] V. Singh, S. Solanki, and P. K. Upadhyay, "Cognitive relaying cooperation in satellite-terrestrial systems with multiuser diversity," *IEEE Access*, vol. 6, pp. 65539–65547, 2018.

[9] W. Liang, S. X. Ng, and L. Hanzo, "Cooperative overlay spectrum access in cognitive radio networks," *IEEE Commun. Surveys Tuts.*, vol. 19, no. 3, pp. 1924–1944, 3rd Quart., 2017.

[10] P. K. Sharma, P. K. Upadhyay, D. B. da Costa, P. S. Bithas, and A. G. Kanatas, "Performance analysis of overlay spectrum sharing in hybrid satellite-terrestrial systems with secondary network selection," *IEEE Trans. Wireless Commun.*, vol. 16, no. 10, pp. 6586–6601, Oct. 2017.

[11] Z. Li, F. Xiao, S. Wang, T. Pei, and J. Li, "Achievable rate maximization for cognitive hybrid satellite-terrestrial networks with AF-relays," *IEEE J. Sel. Areas Commun.*, vol. 36, no. 2, pp. 304–313, Feb. 2018.

[12] W. Cao, Y. Zou, Z. Yang, and J. Zhu, "Relay selection for improving physical-layer security in hybrid satellite-terrestrial relay networks," *IEEE Access*, vol. 6, pp. 65275–65285, 2018.

[13] X. Zhang, K. An, B. Zhang, Z. Chen, Y. Yan, and D. Guo, "Vickrey auction-based secondary relay selection in cognitive hybrid satellite-terrestrial overlay networks with non-orthogonal multiple access," *IEEE Wireless Commun. Lett.*, vol. 9, no. 5, pp. 628–632, May 2020.

[14] X. Zhang, B. Zhang, K. An, Z. Chen, S. Xie, H. Wang, L. Wang, and D. Guo, "Outage performance of NOMA-based cognitive hybrid satellite-terrestrial overlay networks by amplify-and-forward protocols," *IEEE Access*, vol. 7, pp. 85372–85381, 2019.

[15] D.-T. Do and A.-T. Le, "NOMA based cognitive relaying: Transceiver hardware impairments, relay selection policies and outage performance comparison," *Comput. Commun.*, vol. 146, pp. 144–154, Oct. 2019.

[16] T.-L. Nguyen and D.-T. Do, "Power allocation schemes for wireless powered NOMA systems with imperfect CSI: An application in multiple antenna-based relay," *Int. J. Commun. Syst.*, vol. 31, no. 15, p. e3789, Oct. 2018.

[17] D.-T. Do, A.-T. Le, and B. M. Lee, "NOMA in cooperative underlay cognitive radio networks under imperfect SIC," *IEEE Access*, vol. 8, pp. 86180–86195, 2020.

[18] X. Li, J. Li, Y. Liu, Z. Ding, and A. Nallanathan, "Residual transceiver hardware impairments on cooperative NOMA networks," *IEEE Trans. Wireless Commun.*, vol. 19, no. 1, pp. 680–695, Jan. 2020.

[19] D.-T. Do, T.-L. Nguyen, K. M. Rabie, X. Li, and B. M. Lee, "Throughput analysis of multipair two-way replaying networks with NOMA and imperfect CSI," *IEEE Access*, vol. 8, pp. 128942–128953, 2020.

[20] X. Li, M. Liu, C. Deng, P. T. Mathiopoulos, Z. Ding, and Y. Liu, "Full-duplex cooperative NOMA relaying systems with I/Q imbalance and imperfect SIC," *IEEE Wireless Commun. Lett.*, vol. 9, no. 1, pp. 17–20, Jan. 2020.

[21] X. Li, M. Liu, C. Deng, D. Zhang, X.-C. Gao, K. M. Rabie, and R. Kharel, "Joint effects of residual hardware impairments and channel estimation errors on SWIPT assisted cooperative NOMA networks," *IEEE Access*, vol. 7, pp. 135499–135513, 2019.

[22] V. Bankey, V. Singh, and P. K. Upadhyay, "Physical layer secrecy of NOMA-based hybrid satellite-terrestrial relay networks," in *Proc. IEEE Wireless Commun. Netw. Conf. (WCNC)*, Seoul, South Korea, May 2020, pp. 1–6.

[23] T.-L. Nguyen and D.-T. Do, "Exploiting impacts of intercell interference on SWIPT-assisted non-orthogonal multiple access," *Wireless Commun. Mobile Comput.*, vol. 2018, pp. 1–12, Nov. 2018.

[24] D.-T. Do, M.-S.-V. Nguyen, F. Jameel, R. Jantti, and I. S. Ansari, "Performance evaluation of relay-aided CR-NOMA for beyond 5G communications," *IEEE Access*, vol. 8, pp. 134838–134855, 2020.

[25] X. Yan, H. Xiao, C.-X. Wang, and K. An, "Outage performance of NOMA-based hybrid satellite-terrestrial relay networks," *IEEE Wireless Commun. Lett.*, vol. 7, no. 4, pp. 538–541, Aug. 2018.

[26] X. Yan, H. Xiao, C.-X. Wang, and K. An, "On the ergodic capacity of NOMA-based cognitive hybrid satellite terrestrial networks," in *Proc. IEEE/CIC Int. Conf. Commun. China (ICCC)*, Oct. 2017, pp. 1–5.

[27] S. Xie, B. Zhang, D. Guo, and B. Zhao, "Performance analysis and power allocation for NOMA-based hybrid satellite-terrestrial relay networks with imperfect channel state information," *IEEE Access*, vol. 7, pp. 136279–136289, 2019.

[28] Z. Ning, R. Y. K. Kwok, K. Zhang, X. Wang, M. S. Obaidat, L. Guo, X. Hu, B. Hu, Y. Guo, and B. Sadoun, "Joint computing and caching in 5G-envisioned Internet of vehicles: A deep reinforcement learning-based traffic control system," *IEEE Trans. Intell. Transp. Syst.*, early access, Feb. 5, 2020, doi: 10.1109/TITS.2020.2970276.

[29] Z. Ning, K. Zhang, X. Wang, L. Guo, X. Hu, J. Huang, B. Hu, and R. Y. K. Kwok, "Intelligent edge computing in Internet of vehicles: A joint computation offloading and caching solution," *IEEE Trans. Intell. Transp. Syst.*, vol. 22, no. 4, pp. 2212–2225, Apr. 2021, doi: 10.1109/TITS.2020.2997832.

[30] X. Zhang, D. Guo, K. An, Z. Chen, B. Zhao, Y. Ni, and B. Zhang, "Performance analysis of NOMA-based cooperative spectrum sharing in hybrid satellite-terrestrial networks," *IEEE Access*, vol. 7, pp. 172321–172329, 2019.

[31] V. Singh, V. Bankey, and P. K. Upadhyay, "Underlay cognitive hybrid satellite-terrestrial networks with cooperative-NOMA," in *Proc. IEEE Wireless Commun. Netw. Conf. (WCNC)*, Seoul, South Korea, May 2020, pp. 1–6.

[32] V. Singh, P. K. Upadhyay, and M. Lin, "On the performance of NOMA-assisted overlay multiuser cognitive satellite-terrestrial networks," *IEEE Wireless Commun. Lett.*, vol. 9, no. 5, pp. 638–642, May 2020.

[33] K. An, M. Lin, W.-P. Zhu, Y. Huang, and G. Zheng, "Outage performance of cognitive hybrid satellite–terrestrial networks with interference constraint," *IEEE Trans. Veh. Technol.*, vol. 65, no. 11, pp. 9397–9404, Nov. 2016.

[34] N. I. Miridakis, D. D. Vergados, and A. Michalas, "Dual-hop communication over a satellite relay and shadowed rician channels," *IEEE Trans. Veh. Technol.*, vol. 64, no. 9, pp. 4031–4040, Sep. 2015.

[35] Z. Gao, A. Liu, and X. Liang, "The performance analysis of downlink NOMA in LEO satellite communication system," *IEEE Access*, vol. 8, pp. 93723–93732, 2020.

[36] X. Yue, Y. Liu, S. Kang, A. Nallanathan, and Z. Ding, "Exploiting full/half-duplex user relaying in NOMA systems," *IEEE Trans. Commun.*, vol. 66, no. 2, pp. 560–575, Feb. 2018.

[37] A. Abdi, W. C. Lau, M. Alouini, and M. Kaveh, "A new simple model for land mobile satellite channels: First- and second-order statistics," *IEEE Trans. Wireless Commun.*, vol. 2, no. 3, pp. 519–528, May 2003.

[38] J. Hu, G. Li, D. Bian, S. Shi, R. Ge, and L. Gou, "Energy-efficient cooperative spectrum sensing in cognitive satellite terrestrial networks," *IEEE Access*, vol. 8, pp. 161396–161405, 2020.

[39] Z. Ding, M. Peng, and H. V. Poor, "Cooperative non-orthogonal multiple access in 5G systems," *IEEE Commun. Lett.*, vol. 19, no. 8, pp. 1462–1465, Aug. 2015.

[40] S. Arzykulov, G. Nauryzbayev, T. A. Tsiftsis, B. Maham, and M. Abdallah, "On the outage of underlay CR-NOMA networks with detect-and-forward relaying," *IEEE Trans. Cognit. Commun. Netw.*, vol. 5, no. 3, pp. 795–804, Sep. 2019.

[41] I. S. Gradshteyn and I. M. Ryzhik, *Table of Integrals, Series, and Products*, 6th ed. San Diego, CA, USA: Academic, 2000.

ANH-TU LE was born in Lam Dong, Vietnam, in 1997. He is currently pursuing the master's degree in communication and information system with the focus on wireless communication. He is also a Research Assistant with the WICOM Laboratory, which has led by Dr. Thuan. He has authored or coauthored over five technical articles published in peer-reviewed international journals. His research interests include the wireless channel modeling, NOMA, cognitive radio, and MIMO.

NHAT-DUY XUAN HA was born in Gia Lai, Vietnam, in 1996. He is currently a Research Assistant with the WICOM Laboratory. His research interests include the wireless communications, MIMO, cognitive radio, and satellite systems.

DINH-THUAN DO (Senior Member, IEEE) received the B.S., M. Eng., and Ph.D. degrees from Vietnam National University (VNU-HCMC), in 2003, 2007, and 2013, respectively, all in communications engineering. From 2009 to 2010, he was a Visiting Ph.D. Student with the Communications Engineering Institute, National Tsing Hua University, Taiwan. Prior to joining Ton Duc Thang University, he was a Senior Engineer with VinaPhone Mobile Network, from 2003 to 2009. From 2016 to 2020, he was the Founder of the Wireless Communications Research Group funded by Ton Duc Thang University. He was a Supervisor for numerous Ph.D. students in the Ph.D. joint program managed by Ton Duc Thang University and the Technical University of Ostrava (VSB), Czech Republic. His publications include over 95 SCIE-indexed journal articles, one textbook, and five book chapters. His research interests include signal processing in wireless communications networks, NOMA, cognitive radio, physical layer security, reconfigurable intelligent surfaces aided systems, satellite systems, full-duplex transmission, and energy harvesting. He was a recipient of the Golden Globe Award from the Vietnam Ministry of Science and Technology in 2015 (Top ten most excellent scientist nationwide). He served as a Guest Editor for *Annals of Telecommunications* (Springer) Special Issue on "Massive sensors data fusion for health-care informatics" in 2020 and *Physical Communication* (Elsevier) Special Issue on "UAV-enabled B5G/6G networks: emerging trends and challenges" in 2021. He served as a Lead Guest Editor for *Electronics* Special Issue on "Recent advances for 5g: emerging scheme of NOMA in cognitive radio and satellite communications" in 2019 and *International Journal of Distributed Sensor Networks (IJDSN)* Special Issue on "Power domain based multiple access techniques in sensor networks" in 2020. He is currently serving as an Editor for *Computer Communications* (Elsevier) and *KSII Transactions on Internet and Information Systems*. He is also serving as an Associate Editor for *Eurasip Journal on Wireless Communications and Networking* (Springer) and *Electronics*.

SUNEEL YADAV (Member, IEEE) received the B.Tech. degree in electronics and communication engineering from the Meerut Institute of Engineering and Technology, Meerut, India, in 2008, the M.Tech. degree in digital communications from the ABV-Indian Institute of Information Technology and Management, Gwalior, India, in 2012, and the Ph.D. degree in electrical engineering with the IIT Indore, Indore, India, in 2016. He is currently working with the Department of Electronics and Communication Engineering, Indian Institute of Information and Technology Allahabad, Prayagraj, India, as an Assistant Professor, where he is serving as a Faculty-in-Charge of the Mobile and Wireless Networking Laboratory (MoWiNeT). He has numerous publications in peer-reviewed journals and conferences. His current research interests include wireless relaying techniques, cooperative communications, cognitive relaying networks, device-to-device communications, reconfigurable intelligent surfaces, signal processing, physical layer security, and MIMO systems. He served as a TPC member, the session chair, the program co-chair, and a reviewer for various national and international conferences. He is also serving as a reviewer in a number of international journals, including the IEEE Transactions on Vehicular Technology, the IEEE Communications Letters, the IEEE Transactions on Communications, the IEEE Transactions on Information Forensics and Security, the IEEE Systems Journal, IEEE Access, the IEEE Internet of Things Journal, the IEEE Transactions on Signal and Information Processing Over networks, and the *Physical Communication*.

BYUNG MOO LEE (Senior Member, IEEE) received the Ph.D. degree in electrical and computer engineering from the University of California, Irvine, CA, USA, in 2006.

He is currently an Associate Professor with the Department of Intelligent Mechatronics Engineering, Sejong University, Seoul, South Korea. Prior to joining Sejong University, he had ten years of industry experience, including research positions with the Samsung Electronics Seoul R&D Center, the Samsung Advanced Institute of Technology, and the Korea Telecom R&D Center. During his industry experience, he participated in IEEE 802.16/11, Wi-Fi Alliance, 3GPP LTE standardizations, Mobile VCE, and Green Touch Research Consortiums, where he made numerous contributions and filed a number of related patents. His research interests include wireless communications, signal processing, and machine learning applications. From 2015 to 2016, he served as the Vice Chairman for the Wi-Fi Alliance Display MTG.

● ● ●